Reference: *Biol. Bull.* **207:** 56–66. (August 2004)

Cytoskeletal Organization of *Limulus* Amebocytes Pre- and Post-Activation: Comparative Aspects

MARA CONRAD, JOANNA DENOBILE, IRINA CHAIKHOUTDINOV, DOUGLAS ESCRIBANO, KYENG-GEA LEE, AND WILLIAM D. COHEN*

Department of Biological Sciences, Hunter College, New York, NY, and the Marine Biological Laboratory, Woods Hole, Massachusetts

Abstract. One of the major functions of circulating *Limulus* amebocytes is to effect blood coagulation upon receipt of appropriate signals. However, the hypothesis that *Limulus* amebocytes are fundamentally similar to vertebrate thrombocytes and platelets has not been tested sufficiently in previous studies of their cytoskeletal organization. Whereas the earlier data were derived from transmission electron microscopy (TEM) of thin sections of a limited number of cells, improved fluorescence labeling methods that retain cell morphology have now enabled us to survey F-actin and microtubule organization in intact individual amebocytes and in large amebocyte populations pre- and post-activation. Anti-tubulin immunofluorescence showed the marginal band (MB) of microtubules to be ellipsoidal in most unactivated cells, with essentially no other microtubules present. However, minor subpopulations of cells with discoidal or pointed shape, containing corresponding arrangements of microtubules suggestive of morphogenetic intermediates, were also observed. Texas-red phalloidin labeled an F-actin-rich cortex in unactivated amebocytes, accounting for MB and granule separation from the plasma membrane as visualized in TEM thin sections, and supporting earlier models for MB maintenance of flattened amebocyte morphology by pressure against a cortical layer. Shape transformation after activation by bacterial lipopolysaccharide was attributable principally to spiky and spreading F-actin in outer cell regions, with the MB changing to twisted, nuclei-associated forms and eventually becoming unrecognizable. These major pre- and post-activation cytoskeletal features resemble those of platelets and non-mammalian vertebrate thrombocytes, supporting recognition of the *Limulus* amebocyte as a representative evolutionary precursor of more specialized clotting cell types.

Received 30 September 2003; accepted 15 June 2004.

* To whom correspondence should be addressed at Department of Biological Sciences, Hunter College, 695 Park Avenue, New York, NY 10021. E-mail: cohen@genectr.hunter.cuny.edu

Abbreviations: DIC, differential interference contrast; LPS, lipopolysaccharide; MB, marginal band; PBS, phosphate-buffered saline; TEM, transmission electron microscopy.

Introduction

Only a single cell type—the granular amebocyte—is believed to circulate in the hemolymph (blood) of *Limulus polyphemus*, the American horseshoe crab. However, the amebocyte is multifunctional with respect to innate immune mechanisms, playing a role in phagocytosis, wound healing, and clotting (Armstrong, 1985a). In its native, or unactivated, state in the circulation, the amebocyte is a flattened ellipsoid, a characteristic shape maintained by a specialized organization of cytoskeletal elements. When amebocytes are suitably activated, exocytosis occurs, and molecular components released from the intracellular granules cause the hemolymph to clot rapidly (Levin and Bang, 1968; Armstrong and Rickles, 1982). *Limulus* amebocytes are exquisitely sensitive to activation by bacterial lipopolysaccharide (LPS; Armstrong, 1980; Ornberg and Reese, 1981), and algal LPS is also effective (Conrad *et al.*, 2001). Such activation is accompanied by marked changes in cell shape, a feature shared by specialized non-mammalian vertebrate clotting cells (nucleated thrombocytes) and by mammalian platelets (Allen *et al.*, 1979; Debus *et al.*, 1981; Lee *et al.*, 2004). This study was aimed at gauging the extent to which the cytoskeletal characteristics of *Limulus* amebocytes, both pre- and post-activation, are shared by vertebrate thrombocytes and platelets.

The existing relevant data about *Limulus* amebocytes

have been obtained principally by transmission electron microscopy (TEM) of thin sections. Copeland and Levin (1985) described the general fine structure of the native circulating amebocyte, including the nucleus, mitochondria, Golgi apparatus, endoplasmic reticulum, and ribosomes. They also reported that granules of two size classes were present, with "large" ones predominant, and that immature forms of the large granules were Golgi-associated and had distinctive matrix patterns not visible in mature granules. Similar TEM observations were made of the organelles and granules in amebocytes of the Asian horseshoe crab *Tachypleus* (Toh *et al.*, 1991).

Cytoskeletal organization within the *Limulus* amebocyte was also observed in thin sections. Marginal bands (MBs) of microtubules were found in the plane of flattening of unactivated cells by Nemhauser *et al.* (1980), similar to the MBs that are characteristic of nearly all vertebrate nucleated erythrocytes and clotting cells (Fawcett and Witebsky, 1964; Shepro *et al.*, 1966; Behnke, 1970; Jagadeeswaran *et al.*, 1999). Subsequently, Cohen and Nemhauser (1985) suggested that these MBs functioned to maintain the flattened ellipsoidal shape of unactivated cells by interaction with a cortical cytoskeletal network, as in mammalian platelets (Debus *et al.*, 1981). Tablin and Levin (1988)—using a TEM fixation method originally devised to reveal F-actin in platelets (Boyles *et al.*, 1985)—observed thin filament arrays in the cortex of unactivated amebocytes. They suggested that MB interaction with the cortical array might constitute a shape-maintaining cytoskeletal tension system in unactivated cells, similar to that proposed earlier for nucleated erythrocytes by Joseph-Silverstein and Cohen (1984, 1985). They also reported that MBs of activated cells relocated to the cell interior together with cortical filament arrays, and that the MBs never completely disassembled.

The present study had two principal objectives: first, to evaluate earlier proposals that the interaction between the MB and cortical thin filament arrays is responsible for maintaining the shape of unactivated amebocytes; and second, to determine whether post-activation cytoskeletal events in *Limulus* amebocytes parallel those of the more specialized clotting cells of vertebrates. Because the TEM methodology used previously limits depth of field and number of cells that can be observed, we turned to fluorescence labeling. This provides the best assessment of cytoskeletal organization in whole single cells and in large cell populations, and it has been applied successfully to mammalian platelets (Debus *et al.*, 1981). Moreover, impetus for the work came from two recent developments: methods for rapid localization of cytoskeletal proteins with improved retention of native cell shape became available (Lee *et al.*, 2002), and the post-activation cytoskeletal sequence for non-mammalian vertebrate thrombocytes was reported for the first time through use of such methods (Lee *et al.*, 2004).

Employing fluorescence localization, we first examined the features of unactivated *Limulus* amebocytes, focusing on the organization of major cytoskeletal elements: F-actin in the cell cortex, and microtubules in the MBs. Then, after LPS-induced activation, the changes undergone by *Limulus* amebocytes were studied in carefully timed post-activation samples. TEM thin sections of both unactivated and activated amebocytes yielded ancillary details. The results provide a more complete picture of the cellular organization and activities of amebocytes than had been obtained previously, revealing basic structural and functional similarities between these ancient, multifunctional chelicerate blood cells and specialized vertebrate clotting cell types.

Materials and Methods

Living material

Specimens of *Limulus polyphemus* provided by the Marine Resources Center of the Marine Biological Laboratory, Woods Hole, Massachusetts were maintained in the Laboratory's running seawater system at ~16 °C or in closed circulating artificial seawater tanks at ~12 °C, and fed clams or mussels periodically. Individual animals were identified by tape labels or rubber bands attached to the tail.

Preparation of cells for subsequent fluorescence labeling

Unactivated cells. Unactivated cells for population surveys were pre-fixed in suspension by dripping ~0.5 ml of blood directly into 0.5 ml of 2% formaldehyde in 3% NaCl (room temperature, ~23 °C). Subsequent steps were performed by gentle centrifugation of the fixed cells in 2-ml siliconized microcentrifuge tubes. After 5 min of pre-fixation, cells were washed in 3% NaCl; extracted and further fixed for 30 min in 0.6% Brij-58, 2% formaldehyde in 3% NaCl; then washed in PBS and blocked for 1 h in 1% BSA in PBS prior to fluorescence labeling.

Activated cells. Activated cells were prepared by exposure to bacterial LPS as follows. Sterile, virgin, 35-mm plastic petri dishes were prepared for production of successive post-activation time samples. Each dish contained 5 ml of 3% sterile, endotoxin-free NaCl and a sterile LPS-free coverslip (pre-baked >4 h, 200 °C; Armstrong, 1985b). The dishes were pre-chilled for 20 min at ~9 °C to inhibit cell activation. An animal was chilled for 2 h at 4 °C and then dried; after its cephalothorax-opisthosome joint was cleaned with 70% ethanol, it was bled by cardiac puncture with a 20- or 21-gauge needle. With the dishes now placed at room temperature (~23 °C), 1 drop of blood (hemolymph) was added to each dish; the large volume ratio of saline to blood diluted hemolymph components that might otherwise activate the cells. To avoid possible distortion of cell shape, the blood was dripped directly from the open end of a syringe needle into the medium, rather than first drawing blood into

a syringe. The dishes were lightly swirled to disperse the cells, which were then allowed to settle for about 3 min and adhere to coverslips. During this process the cells remained unactivated. To activate the cells and induce exocytosis, 3 ml of supernate were removed *via* LPS-free pipette, and 2 ml of 2× concentrated activating medium (20 m*M* $CaCl_2$, 20 μg/ml LPS in 3% NaCl) was added to each dish, to make final concentrations of 10 m*M* $CaCl_2$ and 10 μg/ml LPS in 3% NaCl. The dishes were incubated at room temperature (~23 °C) and, at particular time points (ranging from 30 s to 10 min), coverslips with adhering amebocytes plus any clot-related material were further processed. Following a wash in 3% NaCl, the material was pre-fixed 5 min in 1% formaldehyde in 3% NaCl, extracted and fixed for 30 min in 3% NaCl containing 0.6% Brij-58 and 2% formaldehyde, washed in PBS, and blocked 1 h in 1% BSA in PBS prior to fluorescence labeling.

Fluorescence labeling and observation of cytoskeletal proteins

To label microtubules, samples were incubated in PBS containing a 50:50 mix of mouse monoclonal anti α- and β-tubulins (Sigma T-9026 and T-4046) that had been pre-bound with Zenon Alexa Fluor 488 F_{ab} (Z-25002, 1:1 by mass; Molecular Probes). For F-actin, samples were incubated in 260 n*M* of Texas-red phalloidin, for a minimum of 10 min, followed by a wash in PBS. Nuclei were labeled with 3 μ*M* DAPI (Sigma D-9542). Labeled samples were examined routinely using a Zeiss phase contrast/epi-fluorescence microscope equipped with a Nikon 950 digital camera; some observations were made using DIC optics.

Preparations for transmission electron microscopy

Sample tubes, each containing 2 ml of 10 μg/ml bacterial lipopolysaccharide (LPS; Sigma) in 3% sterile NaCl, were prepared for various periods: 0 (pre-activation), 30 s, 1 min, 2 min, 5 min, and 10 min. Two drops of blood were added to each tube *via* cardiac puncture, as described above. At each time point, 2 ml of 5% glutaraldehyde in 10 m*M* HEPES (pH 6.8) was added, except for the 0-time tube, to which it was pre-added so that the final glutaraldehyde concentration was ~2.5%. Preparations were fixed for 1 h at room temperature (~23 °C), washed three times in Sorensen's phosphate buffer (0.1 *M*, pH 6.8), and post-fixed in 1% osmium tetroxide in the same phosphate buffer for 1 h. Following three washes in phosphate buffer, the material was dehydrated with ethanol, infiltrated using propylene oxide, and embedded in Epon. Thin sections were cut with a diamond knife, stained with aqueous uranyl acetate and Reynold's lead citrate, and examined in a Hitachi H-600 transmission electron microscope.

Results

Cytoskeletal organization in unactivated cells: fluorescence observations

All of the cells observed in both fresh and fixed blood samples from many animals appeared to be granular amebocytes. As seen by DIC or phase contrast microscopy, the cells were typically flattened, nucleated ovoids, 15–20 μm in length, with 1–2-μm oval, refractile granules packing their cytoplasm (Fig. 1). Anti-tubulin immunofluorescence revealed the MB of unactivated cells as one major circumferential microtubule bundle that conformed to the ellipsoidal cell shape (Fig. 2a, b). The MB was restricted to the plane of flattening (Fig. 2d, e), with few other microtubules visible in the cells (Fig. 2f).

Not all of the cells exhibited this typical ovoid amebocyte morphology, however. A few were circular in profile, and contained a circular MB (Fig. 3a, a′). In addition, in samples from every animal examined, a significant percentage of cells tapered to a point at one or both ends (Fig. 3b–d), and the microtubules in these cells were not organized into typical continuous circumferential MBs but rather extended into the pointed ends (Fig. 3b–3d′). The percentage of pointed amebocytes, as determined by counts of more than 1000 cells in 10 animals, ranged from 1.3% to 8.3% (Table 1). In all cases the predominant variant was singly-pointed; doubly-pointed cells were observed in small numbers and in only five of the animals (Table 1), and cells with circular profile were also observed sporadically.

The distribution of F-actin was determined by Texas-red phalloidin binding (Fig. 4). F-actin appeared in some interior regions of unactivated cells, usually in the vicinity of the nucleus. F-actin was also evident in a thickened cortical layer in edge view throughout the cell periphery (Fig. 4b,

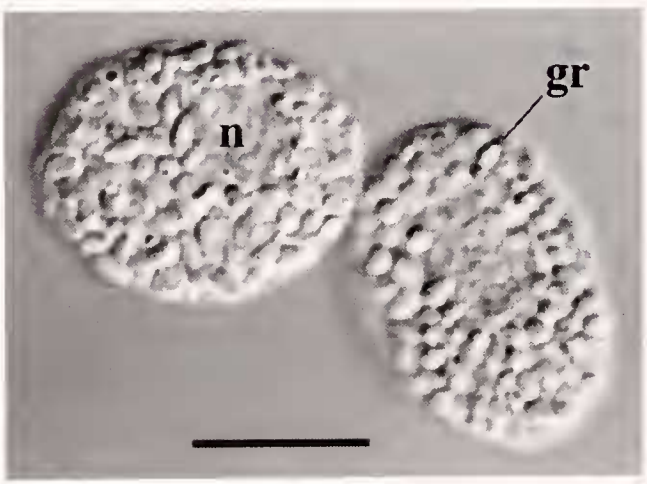

Figure 1. Intact unactivated amebocytes. The cells are flattened ovoids, packed with secretory granules (gr) except in the region occupied by the nucleus (n). DIC image; bar = 10 μm.

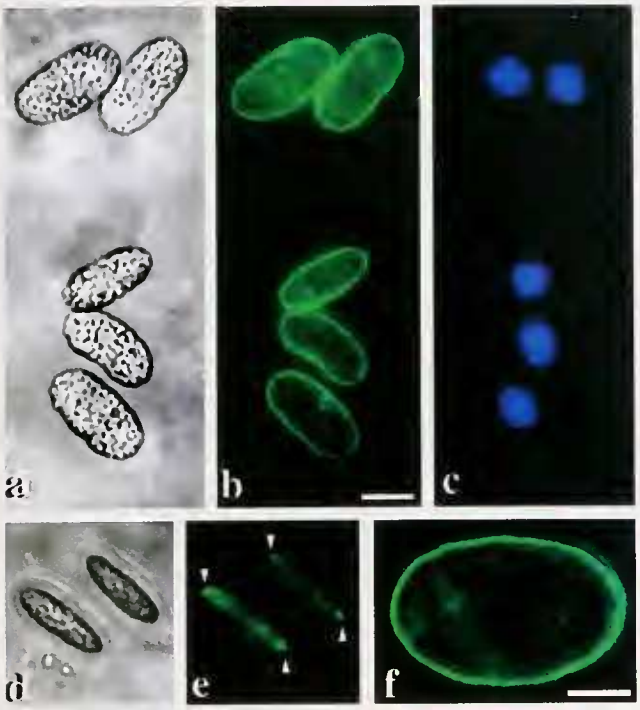

Figure 2. Microtubule distribution in unactivated cells; phase contrast and fluorescence microscopy. (a–c) A field of suspension-labeled cells, observed with phase contrast, anti-tubulin, and DAPI labeling, respectively. The marginal band (MB) in all cells follows ellipsoidal cell contour (a *vs.* b), with nuclei in the interior (c). (d, e) Two cells viewed on edge; phase contrast and anti-tubulin labeling, respectively. Flattened morphology is evident, with MB at the planar extremities (e; arrowheads). (f) Higher magnification view of MB microtubules in another cell. The MB consists of one major circumferential microtubule bundle, with few microtubules evident elsewhere.

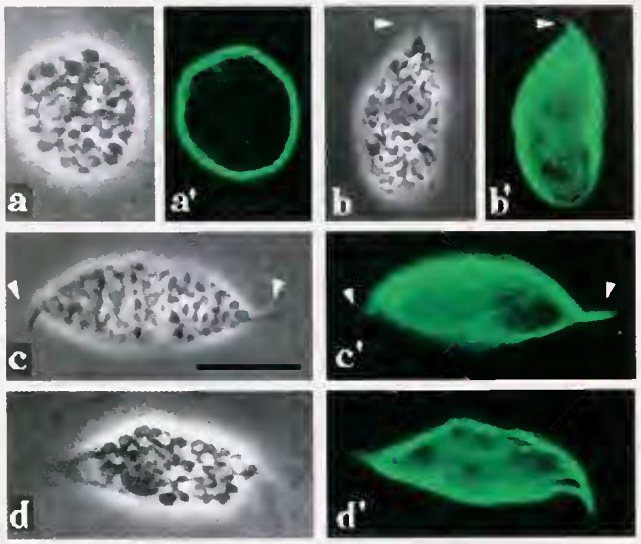

Figure 3. Cytoskeletal variants in the normal unactivated amebocyte population; paired images; phase contrast and fluorescence. (a, a′) Amebocyte, with a circular rather than elliptical profile, and with a circular MB. (b, b′) Singly-pointed amebocyte, with microtubule bundles following the entire cell contour including the pointed tip (arrowheads). This variant type was found in every animal examined (see also Table 1). (c, c′; d, d′) Examples of doubly-pointed cells, with microtubule bundles forming incomplete, doubly-pointed MBs (arrowheads). This variant was found only in some animals. Bar = 10 μm.

arrows), with adjacent hazily labeled areas that are attributable to cortical F-actin being observed in face view.

Additional structural features of unactivated cells: TEM observations

To visualize cytoskeletal elements and cellular organelles in greater detail, fixed, unactivated cells were examined in TEM thin sections (Fig. 5). In addition to the electron-dense granules found throughout the cell, major components visible in survey views included nucleus, mitochondria, and Golgi apparatus; there was no surface-associated canalicular membrane system such as is found in non-mammalian vertebrate thrombocytes and mammalian platelets (Fig. 5a). Examination of numerous mature granules in TEM thin sections showed that those closest to the cell surface were always separated from the plasma membrane by a cytoplasmic gap ~50 nm thick (Fig. 5b, c). At higher magnifications, MB microtubules and centrioles (Fig. 5d–g) were visible, with the MB routinely observed at the cell periphery in various sectional views (*e.g.*, Fig. 5d *vs.* e). In cross sections, the closest approach of MB component microtubules to the plasma membrane was ~50 nm, as in the case of granules (Fig. 5d; arrowheads and white bars).

Centrioles were found regularly, often with both members of a pair in a given section, usually located between the nucleus and Golgi apparatus. Centrioles had classic cylindrical structure, ~0.2 × 0.3 μm, with one closed end (Fig. 5f, arrow) and typical 9 + 0 triplet cross section (Fig. 5g). Centriole pairs were present in both parallel and perpendicular orientation, and when both members of a pair were

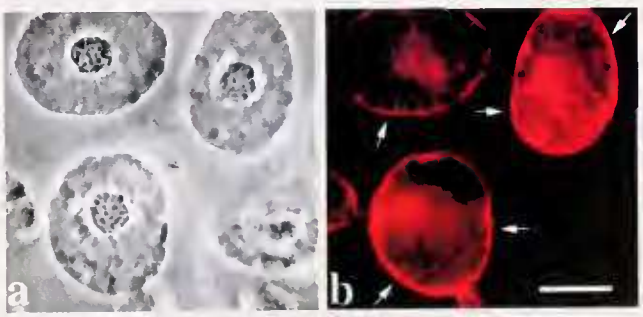

Figure 4. F-actin distribution in unactivated cells; phase contrast and fluorescence microscopy. (a) Phase contrast, several cells with nuclei visible. (b) Same cells as in (a), rhodamine-phalloidin binding by F-actin filaments. F-actin was concentrated principally in regions near the nucleus, and in a cortical layer visible in edge view at the cell periphery (b, arrows). Bar = 10 μm.

Table 1

Percentage of pointed granular amebocytes in hemolymph of 10 animals

Animal no.	No. cells counted	% SP	% DP	Total % pointed
1	1005	3.9	0	3.9
2	1101	6.0	0.6	6.6
3	1348	2.9	0.3	3.2
4	1002	1.3	0	1.3
5	1183	4.5	0.6	5.1
6	1003	8.3	0	8.3
7	1221	4.1	0.2	4.3
8	1037	2.6	0	2.6
9	1137	5.7	1.0	6.7
10	1276	1.8	0	1.8

Key: SP = singly-pointed; DP = doubly-pointed.

Note: Each count was made on more than 1000 cells per animal. Animals were of different sizes and sexes. Cell morphology was preserved by free flow of hemolymph directly into fixative, thus avoiding pipette-induced shearing or contact with slides or coverslips prior to fixation.

present in cross section, their triplets had the same "pinwheel" polarity (Fig. 5g, arrows). Few microtubules were present in the vicinity of the centrioles, which appeared to have no physical connection with the MB.

Cytoskeletal features in LPS-activated cells: fluorescence observations

Anti-tubulin immunofluorescence was used to follow the fate of marginal band microtubules after activation (Fig. 6). At $t = 30$ s the MB was visible at the periphery, but appeared buckled and otherwise distorted in shape (Fig. 6a, a′). At 3 min it was still recognizable, but now highly twisted and physically associated with the nucleus (Fig. 6b). At 7 min the MB was still nucleus-associated but nearly unrecognizable (Fig. 6c, c′), and ultimately it disappeared as such, though some tubulin-containing areas were visible (Fig. 6d, d′).

F-actin was redistributed in a dramatic way following activation (Fig. 7). Shortly after activation, cytoplasmic F-actin content increased in the cell population ($t = 1$ min; Fig. 7a″), while MB microtubules were still visible in distinct but twisted bundles (Fig. 7a′, arrow). At ~5 min, with MBs less distinct, many cells had spiky F-actin-rich protrusions several micrometers in length (Fig. 7b″). At 7 min, the spiky exterior of cells in some regions of the clot was less pronounced, and the F-actin had spread into more circular patterns (Fig. 7c″). However, not all cells responded in this way; at $t = 10$ min, with distinct microtubule bundles no longer present, cells in other clot regions still had numerous long F-actin-containing filopodia that appeared to cross and perhaps touch those of adjacent cells (Fig. 7d″).

Additional structural features of LPS-activated cells: TEM observations

Extensive nuclear deformation and reshaping was evident in thin sections of many cells in clots several minutes after activation (Fig. 8a). Microtubule bundles were no longer seen at the cell periphery, as they were in unactivated amebocytes, but bundles of microtubules were consistently found adjacent to the deformed nuclei (Fig. 8b, arrows). In no instance was a complete internalized MB observed, however. Centrioles remained intact, even in fully exocytosed cells (Fig. 8c), but there was no evidence of centrosomal microtubule organization in their vicinity.

Discussion

Our observations of unactivated amebocyte structure—as revealed by fluorescence localization of microtubules and F-actin—support earlier proposals that a cortical F-actin layer and the marginal band (MB) function together to maintain the shape of these cells. In addition, the cytoskeletal variants that we detected for the first time in the native cell population suggest that biogenesis of *Limulus* amebocytes involves microtubule-based mechanisms similar to those in other MB-containing blood cell types, such as the nucleated erythrocytes of non-mammalian vertebrates. Moreover, although *Limulus* amebocytes are multifunctional, activation by bacterial LPS produces major changes in their cytoskeletal organization that are closely similar to those occurring in vertebrate thrombocytes and mammalian platelets. Each of these points is further discussed below.

The cytoskeleton of unactivated cells

As observed previously by TEM (Nemhauser *et al.*, 1980), unactivated amebocytes have a MB of microtubules in their plane of flattening. In the present work, the MB was readily visualized by combining brief pre-fixation, detergent extraction, and immunofluorescence with Zenon-prelabeled anti-tubulin (Lee *et al.*, 2002). The MB matched the contour of each cell in the plane of flattening (*e.g.*, Fig. 2a–e), and essentially no microtubules were observed elsewhere in the unactivated cell (Fig. 2f).

TEM thin sections revealed a space ~50 nm wide separating both MB and granules from the plasma membrane bilayer (Fig. 5b, c, d). A comparable gap occurs between MB and plasma membrane in granular lobster hemocytes (Cohen *et al.*, 1983), and between the dense granules and plasma membrane of unactivated ("resting") platelets, which fuse only after activation (Morgenstern, 1995). This is evidence of a cortical layer throughout the entire unactivated cell, as illustrated diagrammatically in Figure 9, corresponding to a filamentous layer underlying the plasma membrane, as observed previously in thin sections of ame-

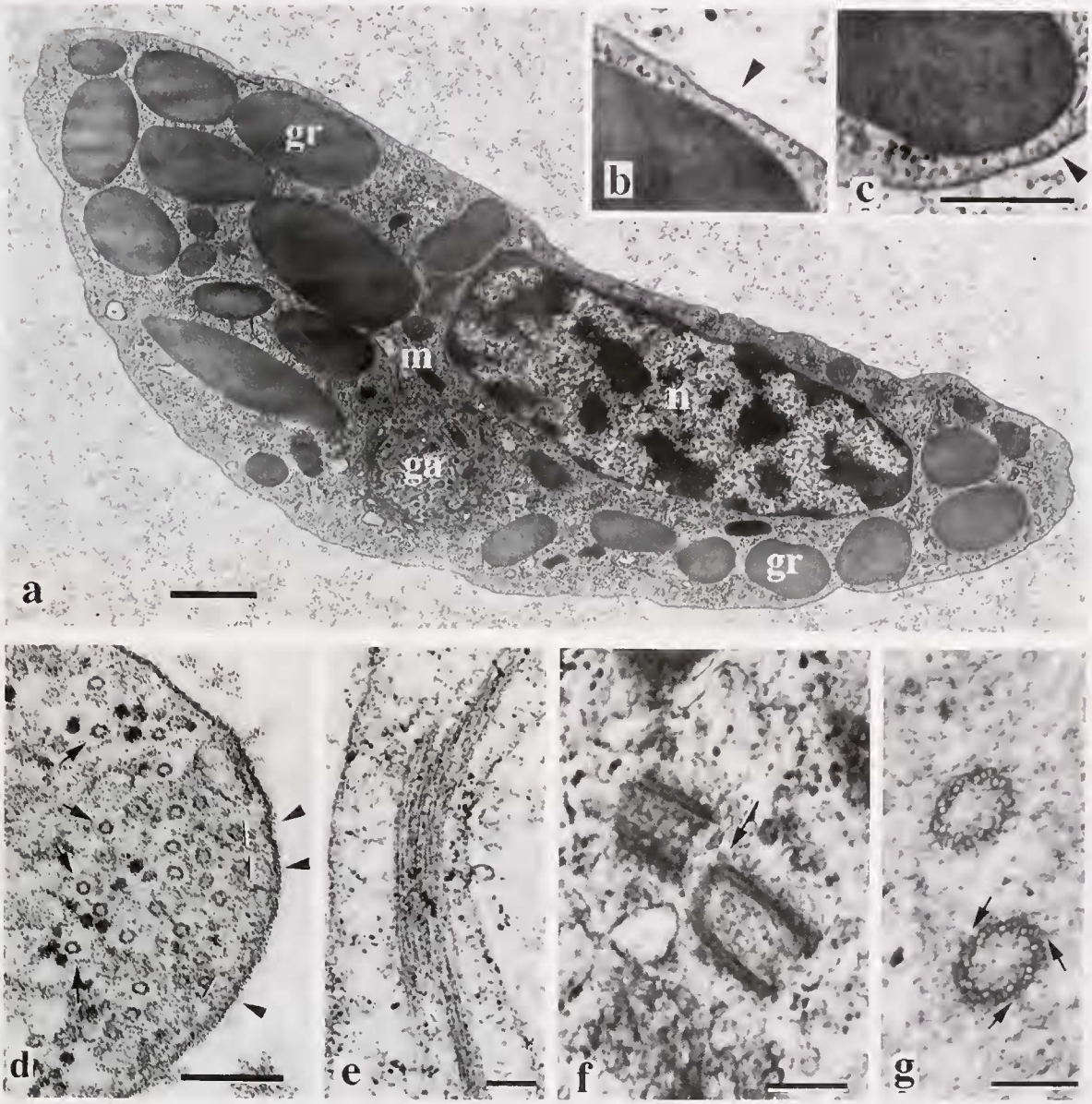

Figure 5. Structure of unactivated cells, TEM thin sections. (a) Longitudinal section overview, showing granules (gr), Golgi apparatus (ga), nucleus (n), mitochondria (m). Note: background material external to cell = fixed hemocyanin. (b, c) Enlarged views of gr-labeled granules in the same cell, showing the granules separated from the plasma membrane by a gap of ~50 nm (arrowheads). (d) Marginal band (MB) of microtubules in cross section, with some of the interior microtubules indicated by arrows; like granules, the outermost MB microtubules of unactivated cells are separated from the plasma membrane by a gap of ~50 nm, as indicated by the white lines (opposite arrowheads). (e) MB microtubules in longitudinal section. (f, g) Centriole pairs, shown in longitudinal and cross section, respectively, are a common feature. Longitudinal view shows typical closure at one end (f, arrow), and the triplet "pinwheel" directionality of pairs is evident in cross-sectional view (g, arrows). Bars: (a) = 1 μm; (b, as in c) = 0.5 μm; (d–g) = 0.2 μm.

bocytes prepared by freeze-substitution (Ornberg, 1985), or by a fixation method that preserves cortical F-actin in platelets (Boyles *et al.*, 1985; Tablin and Levin, 1988).

Because of its binding specificity, phalloidin labeling verifies that an F-actin-rich cortical layer is present in the *Limulus* amebocyte (Fig. 4), as shown previously for F-actin in unactivated platelets and vertebrate thrombocytes (Debus *et al.*, 1981; Lee *et al.*, 2004). Thus, in the *Limulus* amebocyte, the MB appears to act as a flexible frame that maintains unactivated cell shape by pressing from within against an actin-rich, filamentous cortical network (Fig. 9), in agreement with earlier proposals based on thin sections

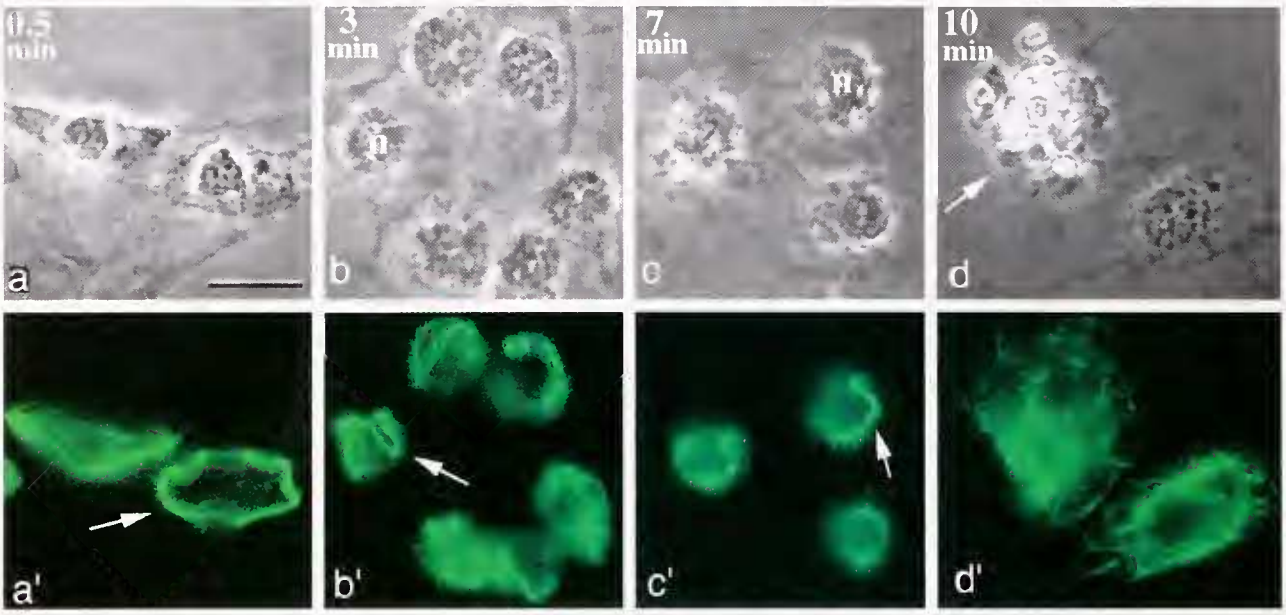

Figure 6. Time-course of microtubule redistribution during clot formation by lipopolysaccharide-activated amebocytes, observed by anti-tubulin immunofluorescence (phase contrast-fluorescence pairs; time of fixation is in upper left corner of phase images a–d). (a, a′) Cells 30-s post-activation; MBs are still at the periphery, somewhat folded and buckled, but still recognizable (*e.g.*, a′, arrow); most granules have already exocytosed, and boundaries of individual cells are beginning to be obscured by the clot as viewed in phase contrast (a). (b, b′) 3 min after activation; microtubules have moved into the interior and are associated with nuclei; many MBs are still recognizable as highly twisted forms (*e.g.*, arrow). (c, c′) 7 min post-activation; MBs are essentially unrecognizable as such, but microtubule bundles are still localized at nuclear surfaces (n; arrow in c′). (d, d′) 10 min post-activation; microtubules have a much more diffuse distribution, even in the few remaining cells in which exocytosis is incomplete (d, arrow). Bar = 10 μm.

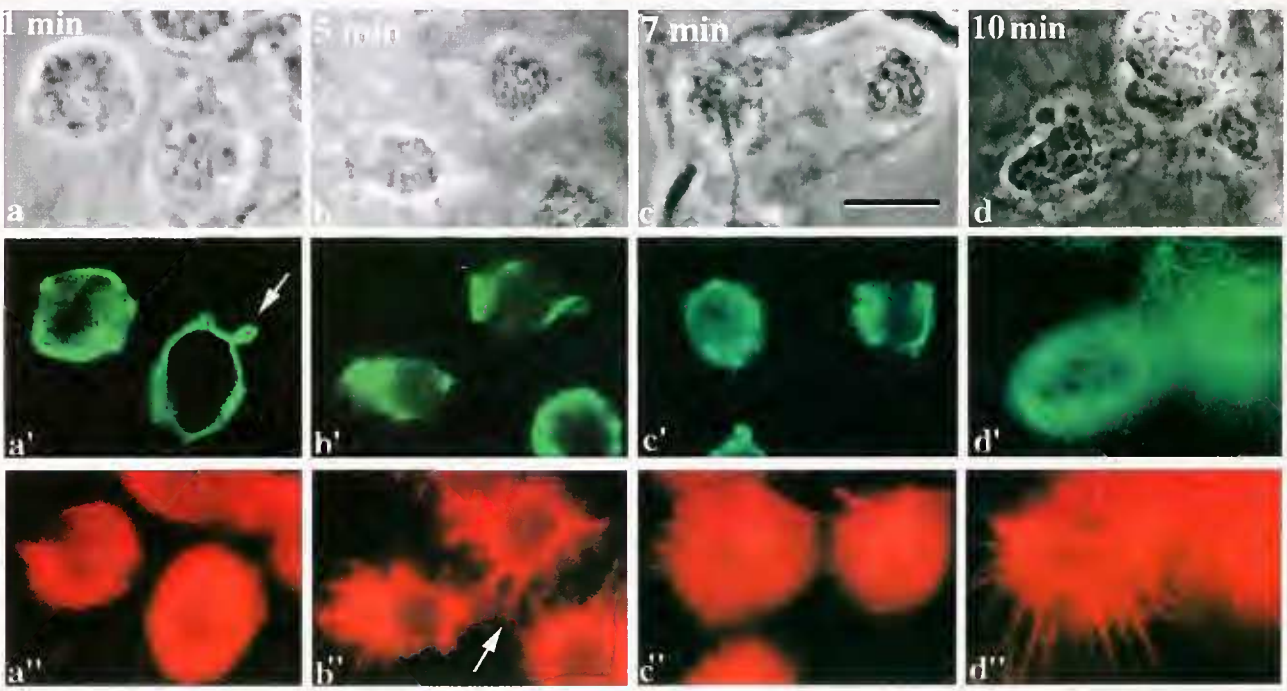

Figure 7. Activation time-course for F-actin redistribution relative to microtubules during clot formation, observed by anti-tubulin and rhodamine-phalloidin fluorescence (phase contrast-fluorescence triplets); time of fixation is in upper left corner of phase micrographs (a–d). Individual cells are not discernible in phase contrast post-activation, with the image mottled by the surrounding clot. (a–a″) t = 1 min; exocytotic cells within the clot have become more compact, with marginal bands (MBs) beginning to deform and twist (a′, arrow) and cytoplasmic F-actin distribution in a variable phase (a″). (b–b″) t = 5 min; MBs are twisted and located in the interior, closer to nuclei (b′); spiky F-actin-rich protrusions appear on most cells (b″, arrow). (c–c″) t = 7 min; MBs have lost recognizability, and microtubule bundles remain in the interior close to nuclei (c′); F-actin has redistributed in a spreading cell pattern, with a few peripheral F-actin-rich protrusions remaining (c″). (d–d″) t = 10 min; some variation was noted in different regions of the clot, with this region still containing cells that had long F-actin-rich filopodia. Bar = 10 μm.

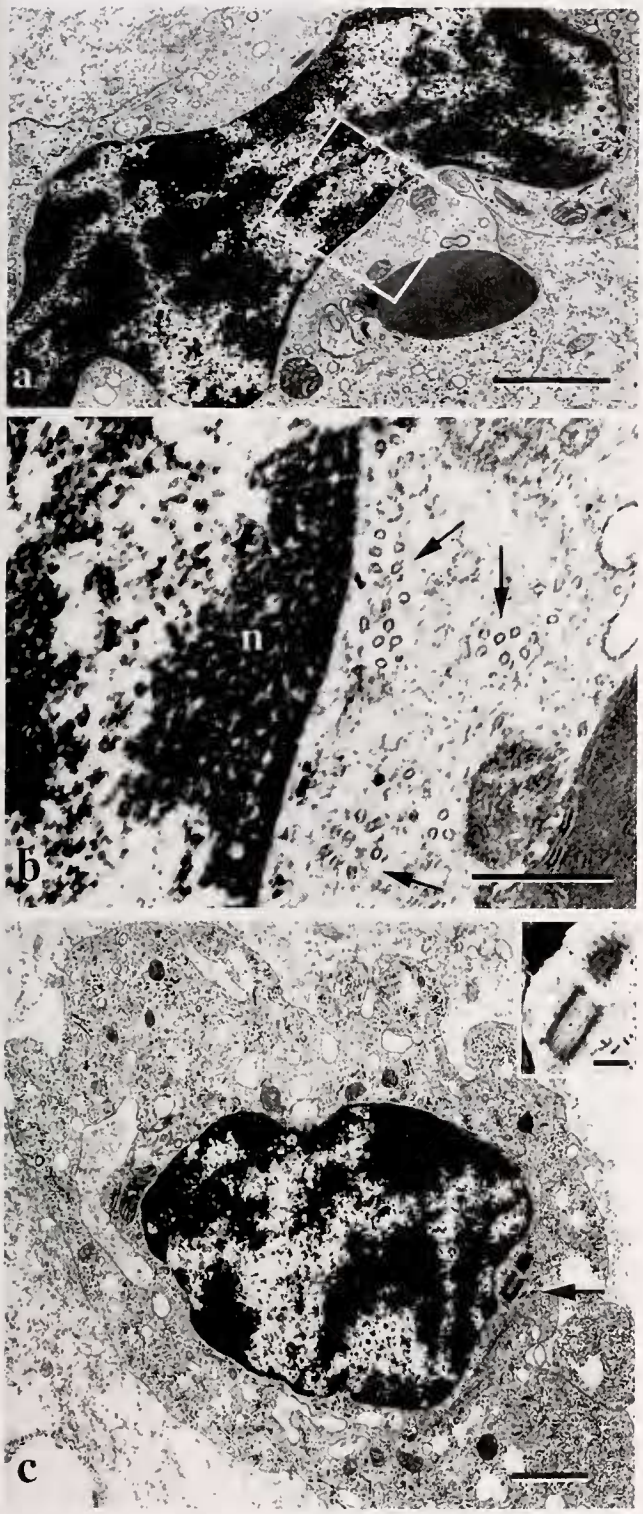

Figure 8. Cytoskeletal and nuclear structure in lipopolysaccharide-activated cells (TEM). (a) ~5 min post-activation; low-magnification view of deformed nucleus. (b) Higher magnification view of area delimited in (a), showing bundles of microtubules adjacent to nucleus (arrows). (c) ~10 min post-activation; exocytosis is complete, with no intact granules remaining. Centrioles (arrow, and inset) remain intact. Bars: (a, c) = 1 μm; (b) = 0.25 μm; (c inset) = 0.2 μm.

(Nemhauser *et al.*, 1980; Cohen and Nemhauser, 1985; Tablin and Levin, 1988). The same mechanism applies to platelets and to non-mammalian thrombocytes (Lee *et al.*, 2004), and it is similar to that proposed previously for the MB-containing nucleated erythrocytes of all non-mammalian vertebrates (Joseph-Silverstein and Cohen, 1984, 1985).

There is, however, one fundamental difference between the MB-containing cytoskeleton of unactivated nucleated erythrocytes and that of invertebrate or vertebrate clotting cells. The erythrocyte system is designed for long-term maintenance of circulating cell shape, with the MB interacting with a filamentous network—the actin-spectrin membrane skeleton—that is highly specialized for stability. In contrast, the cortical layer of the clotting cell—through interaction with the MB—must maintain the unactivated circulating shape for long periods, while remaining at all times responsive to the signals that induce the rapid shape transformations associated with clotting. As shown in the current work with *Limulus* amebocytes, as well as in previous work on platelets and non-mammalian vertebrate thrombocytes, the ultimate effector targeted by such signaling appears to be F-actin.

Unactivated cytoskeletal variants

The presence of minor numbers of discoidal cells containing discoid MBs and pointed cells containing a pointed microtubular cytoskeleton (Fig. 3) raises the possibility that there is more than one blood cell type in *Limulus*. While such amebocytes have not been reported previously, two hemocyte types—granular and nongranular—have been de-

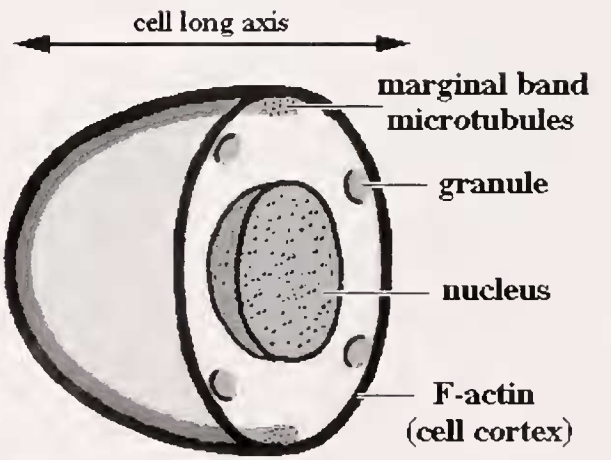

Figure 9. Diagrammatic summary of cytoskeletal features of the unactivated *Limulus* amebocyte; cutaway view with cell thickness exaggerated). The marginal band (MB), enclosed within the F-actin-rich cortical layer in the plane of flattening, is presumed to act as a flexible frame imposing pressure against the cortex to maintain the flattened ellipsoidal shape of unactivated cells. Both the MB and the most peripheral mature granules abut the cortical layer, as illustrated in the cross-sectional view.

scribed for the Asian horseshoe crab *Tachypleus* (Toh *et al.*, 1991). Nongranular hemocytes have not been observed in *Limulus*, but the singly-pointed granular cells constituted ~1%–8% of the population in 10 animals examined, with a few doubly-pointed ones in some (Table 1). Their number and constancy in samples prepared by free flow of blood directly into fixative preclude simple dismissal as a surface-contact or pipetting artifact, but it is highly unlikely that they represent a different cell type. Both singly-pointed and doubly-pointed morphologies (Fig. 3) are reminiscent of forms found previously during MB biogenesis in developing amphibian erythroblasts *in vivo* and *in vitro* (Ginsburg *et al.*, 1989; Twersky *et al.*, 1995; Huang *et al.*, 2001). In addition, discoidal amphibian erythrocytes containing discoidal MBs are reported to precede the generation of ellipsoids (Dorn and Broyles, 1982). Thus the observed variant amebocyte types may be biogenetic intermediates in the formation of ovoid *Limulus* amebocytes. Alternatively, pointed morphology could be produced by mechanically deteriorating cytoskeletons in older cells destined for retirement, and both possibilities remain to be tested. Unfortunately, this problem is made difficult because the sites of amebocyte production and recycling in the adult animal are still unknown.

Post-activation events

Shortly after activation, the MB remained associated with the cell periphery, still with few microtubules evident elsewhere (Fig. 6a, a′). Within a few minutes, however, the MB rapidly lost this association, as twisted microtubule bundles moved to the interior, adjacent to cell nuclei (Fig. 6b, b′, c, c′). In TEM thin sections, these interior bundles of microtubules were consistently found near the nuclear indentations of activated cells (Fig. 8a, b), suggesting that they may be responsible for altering nuclear shape. Though not commonly observed in other systems, microtubule association with nuclear constrictions occurs both in activated non-mammalian thrombocytes (Lee *et al.*, 2004) and in cultured leukemic cells undergoing apoptosis (Pittman *et al.*, 1997). Microtubule function in nuclear remodeling is perhaps best documented for the spermatid manchette in a mechanism involving dynein and kinesin motor proteins (McIntosh and Porter, 1967; Hall *et al.*, 1992), but in the other cases the effector mechanism is unknown. In the activated *Limulus* amebocytes, all recognizable MB microtubules disappeared eventually (Fig. 6d′; Fig. 7d′), in this respect resembling lobster hemocytes spreading on a substrate (Cohen *et al.*, 1983).

Following activation induced by lipopolysaccharide (LPS), the F-actin reorganized and spread outward, producing long, spiky, F-actin-rich filopodia as a major feature (Fig. 7a″ *vs.* 7b″, d″). Though not previously shown to contain F-actin, such spiky filopodia have also been observed in individual LPS-activated spheroidal amebocytes separated on a substratum—that is, not in a clot (Armstrong, 1985a). Thus, formation of such spiky filopodia does not require cell-cell contact. The F-actin in cells in some regions of our clots transformed into flattened discoidal patterns similar to individual surface-spreading non-mammalian vertebrate thrombocytes (Lee *et al.*, 2004) and mammalian blood platelets (Allen *et al.*, 1979). However, in other regions the cells retained spiky F-actin filopodia for longer periods, possibly contributing to the integrity and mechanical properties of the clot, as proposed for platelets (Cohen, 1979). Lack of synchrony or identity in the response of cells throughout the clot is not surprising, since the clots formed *in vitro* had local variations in thickness, cell density, and cell proximity to the clot surface and the surrounding medium.

In contrast to the outward-moving F-actin, the microtubules relocated into the interior and became associated with nuclei (Figs. 6b′, 7b′), in agreement with TEM observations of Tablin and Levin (1988), and in marked similarity to fluorescently localized F-actin and microtubules in activated non-mammalian thrombocytes and in platelets (Debus *et al.*, 1981; Lee *et al.*, 2004). These results support the hypothesis that the microtubules function primarily in the biogenesis and maintenance of unactivated amebocyte morphology, whereas F-actin is involved primarily in motile and morphogenetic functions associated with post-activation shape transformation. Thus, in most respects, the function of major cytoskeletal elements before and after activation of *Limulus* amebocytes closely resembles that of both mammalian blood platelets and non-mammalian nucleated thrombocytes (Allen *et al.*, 1979; Debus *et al.*, 1981; Lee *et al.*, 2004).

With respect to signaling pathways involved in *Limulus* amebocyte exocytotic and cytoskeleton-based activity, some cells that had undergone complete exocytosis were found to contain twisted but nearly intact MBs (*e.g.*, Figs. 6a,′ 7a′). This indicates that MB disorganization *per se* is not a prerequisite for exocytosis. Conversely, complete exocytosis is not a prerequisite for complete MB disorganization (*e.g.*, Fig. 6d, arrow). Thus, bacterial LPS probably triggers several sequences of events that proceed in parallel, but are relatively independent of each other.

Amebocyte multifunctionality

Centrioles were observed in thin sections of unactivated cells with such frequency that we assume a centriole pair to be present in every cell. What might their function be in mature amebocytes? They are not involved in cell division, as mitosis has been observed only in immature amebocyte precursors in early *Limulus* embryos (Coursey *et al.*, 2003), and never in amebocytes of adult animals (*e.g.*, Copeland and Levin, 1985). They are not associated with MB micro-

tubules as in molluscan erythrocytes, in which centrioles function in MB reassembly (Nemhauser *et al.*, 1983), and there are few other cytoplasmic microtubules present. Moreover, the centrioles remain adjacent to the nucleus in cells in which exocytosis is complete (Fig. 8c), with no evidence of centrosomal microtubule nucleation during that process. Are they just "leftovers" from poles of the last mitotic spindle preceding their biogenesis? Not necessarily. As their name suggests, *Limulus* amebocytes are multifunctional cells that can move about the tissues of the animal with pseudopodia, in addition to being carried by the circulation; and they can also engage in limited phagocytosis independent of exocytosis and clotting (Armstrong, 1985a). Centriole-containing centrosomes may well be involved in these activities, as in similar crawling movements of mammalian polymorphonuclear leukocytes and T-cells (Zigmond, 1978; Pryzwansky *et al.*, 1983; Volkov *et al.*, 1998; Abal *et al.*, 2002).

Our TEM thin section observations (Fig. 5) confirmed the general organelle and granule content observed in earlier studies (Copeland and Levin, 1985), as well as the absence of a subsurface membranous canalicular system such as is characteristic of both non-mammalian vertebrate thrombocytes and platelets (*e.g.*, White and Clawson, 1980; Daimon and Uchida, 1985). Why are canaliculi not present in the *Limulus* amebocyte? The canalicular system is a specialized compartment that responds to clotting activation signals by rapid reorganization, and we suggest that the canaliculi of clotting cells represent a degree of differentiation incompatible with the multifunctionality of *Limulus* amebocytes. This raises an important issue with respect to mechanisms of innate immunity and comparative hematology. There appear to be two evolutionary strategies at work: (a) several functions can be encompassed within a single cell type, in which case the cell must be sensitive to a variety of signals and respond to them in various specialized ways *via* separate paths; or (b) functions can be distributed among more specialized cell types, with correspondingly specialized signal receptor systems and fewer intracellular pathways. The *Limulus* amebocyte exemplifies the former, whereas the presence of canaliculi in vertebrate thrombocytes and platelets is symptomatic of the latter.

Acknowledgments

This work was supported by grants from the City University of New York (PSC-CUNY 63215), the Howard Hughes Medical Institute (HHMI) Undergraduate Science Education Program 71100-534602), and the National Science Foundation (NSF 9808368). Special thanks go to Dr. Peter Armstrong, to the reviewers, and to Editor-in-Chief Michael J. Greenberg for substantial scientific and editorial input. This work is a contribution from the Comparative Hematology and Innate Immunity Cluster (CHIIC) of the MBL's Whitman Center.

Literature Cited

Abal, M., M. Piel, V. Bouckson-Castaing, M. Mogensen, J. B. Sibarita, and M. Bornens. 2002. Microtubule release from the centrosome in migrating cells. *J. Cell Biol.* **159:** 731–737.

Allen, R. D., L. R. Zacharski, S. T. Widirstky, R. Rosenstein, L. M. Zaitlin, and D. R. Burgess. 1979. Transformation and motility of human platelets: details of the shape change and release reaction observed by optical and electron microscopy. *J. Cell Biol.* **83:** 126–142.

Armstrong, P. B. 1980. Adhesion and spreading of *Limulus* blood cells on artificial surfaces. *J. Cell Sci.* **44:** 243–262.

Armstrong, P. B. 1985a. Adhesion and motility of the blood cells of *Limulus*. Pp. 77–124 in *Blood Cells of Marine Invertebrates*, W. D. Cohen, ed. Alan R. Liss, New York.

Armstrong, P. B. 1985b. Amebocytes of the American "horseshoe crab," *Limulus polyphemus:* a practical guide. Pp. 253–258 in *Blood Cells of Marine Invertebrates*, W. D. Cohen, ed. Alan R. Liss, New York.

Armstrong, P. B., and F. R. Rickles. 1982. Endotoxin-induced degranulation of the *Limulus* amebocyte. *Exp. Cell Res.* **140:** 15–24.

Behnke, O. 1970. A comparative study of microtubules of disk-shaped blood cells. *J. Ultrastruct. Res.* **31:** 61–75.

Boyles, J., J. E. Fox, D. R. Phillips, and P. E. Stenberg. 1985. Organization of the cytoskeleton in resting, discoid platelets: preservation of actin filaments by a modified fixation that prevents osmium damage. *J. Cell Biol.* **101:** 1463–1472.

Cohen, I. 1979. The contractile system of blood platelets and its function. *Methods Achiev. Exp. Pathol.* **9:** 40–86.

Cohen, W. D., and I. Nemhauser. 1985. Marginal bands and the cytoskeleton in blood cells of invertebrates. Pp. 3–49 in *Blood Cells of Marine Invertebrates*, W. D. Cohen, ed. Alan R. Liss, New York.

Cohen, W. D., I. Nemhauser, and M. F. Cohen. 1983. Marginal bands of lobster blood cells: disappearance associated with changes in cell morphology. *Biol. Bull.* **164:** 50–61.

Copeland, D. E., and J. Levin. 1985. The fine structure of the amebocyte in the blood of *Limulus polyphemus*. I. Morphology of the normal cell. *Biol. Bull.* **169:** 449–457.

Conrad, M. L., R. L. Pardy, and P. B. Armstrong. 2001. Response of the blood cell of the American horseshoe crab, *Limulus polyphemus*, to a lipopolysaccharide-like molecule from the green alga *Chlorella*. *Biol. Bull.* **201:** 246–247.

Coursey, Y., N. Ahmad, B. M. McGee, N. Steimel, and M. Kimble. 2003. Amebocyte production begins at stage 18 during embryogenesis in *Limulus polyphemus*, the American horseshoe crab. *Biol. Bull.* **204:** 21–27.

Daimon, T., and K. Uchida. 1985. Ultrastructural evidence of the existence of the surface connected canalicular system in the thrombocyte of the shark (*Triakis scyllia*). *J. Anat.* **141:** 193–200.

Debus, E., K. Weber, and M. Osborn. 1981. The cytoskeleton of blood platelets viewed by immunofluorescence microscopy. *Eur. J. Cell Biol.* **24:** 45–52.

Dorn, A. R., and R. H. Broyles. 1982. Erythrocyte differentiation during the metamorphic hemoglobin switch of *Rana catesbeiana*. *Proc. Natl. Acad. Sci. USA* **79:** 5592–5596.

Fawcett, D. W., and F. Witebsky. 1964. Observations on the ultrastructure of nucleated erythrocytes and thrombocytes with particular reference to the structural basis of their discoidal shape. *Z. Zellsforsch. Mirosk. Anat.* **62:** 785–806.

Ginsburg, M. F., L. H. Twersky, and W. D. Cohen. 1989. Cellular

morphogenesis and the formation of marginal bands in amphibian splenic erythroblasts. *Cell Motil. Cytoskel.* **12:** 157–168.

Hall, E. S., J. Eveleth, C. Jiang, D. M. Redenbach, and K. Boekelheide. 1992. Distribution of the microtubule-dependent motors cytoplasmic dynein and kinesin in rat testis. *Biol. Reprod.* **46:** 817–828.

Huang, L-F., L. Levinhar, K-G. Lee, M. Ginsburg, and W. D. Cohen. 2001. *In vitro* morphogenesis of amphibian erythroblasts. *Cell Biol. Internat.* **25:** 1229–1236.

Jagadeeswaran, P., J. P. Sheehan, F. E. Craig, and D. Troyer. 1999. Identification and characterization of zebrafish thrombocytes. *Br. J. Haematol.* **107:** 731–738.

Joseph-Silverstein, J., and W. D. Cohen. 1984. The cytoskeletal system of nucleated erythrocytes. III. Marginal band function in mature cells. *J. Cell Biol.* **98:** 2118–2125.

Joseph-Silverstein, J., and W. D. Cohen. 1985. Role of the marginal band in an invertebrate erythrocyte: evidence for a universal mechanical function. *Can. J. Biochem. Cell Biol.* **63:** 621–630.

Lee, K-G., A. Braun, I. Chaikhoutdinov, J. DeNobile, M. Conrad, and W. D. Cohen. 2002. Rapid visualization of microtubules in blood cells and other cell types in marine model organisms. *Biol. Bull.* **203:** 204–206.

Lee, K-G, T. Miller, I. Anastassov, and W. D. Cohen. 2004. Shape transformation and cytoskeletal reorganization in activated non-mammalian thrombocytes. *Cell Biol. Internat.* **28:** 299–310.

Levin, J., and F. B. Bang. 1968. Clottable protein in *Limulus*; its localization and kinetics of its coagulation by endotoxin. *Thromb. Diath. Haemorrh.* **19:** 186–197.

McIntosh, J. R., and K. R. Porter. 1967. Microtubules in the spermatids of the domestic fowl. *J. Cell Biol.* **35:** 153–173.

Morgenstern, E. 1995. The formation of compound granules from different types of secretory organelles in human platelets (dense granules and alpha-granules). A cryofixation/-substitution study using serial sections. *Eur. J. Cell Biol.* **68:** 183–190.

Nemhauser, I., R. Ornberg, and W. D. Cohen. 1980. Marginal bands in blood cells of invertebrates. *J. Ultrastruct. Res.* **70:** 308–317.

Nemhauser, I., J. Joseph-Silverstein, and W. D. Cohen. 1983. Centrioles as microtubule organizing centers for the marginal band of a molluscan erythrocyte. *J. Cell Biol.* **86:** 286–291.

Ornberg, R. L. 1985. Exocytosis in *Limulus* amebocytes. Pp. 127–142 in *Blood Cells of Marine Invertebrates,* W. D. Cohen, ed. Alan R. Liss, New York.

Ornberg, R. L., and T. S. Reese. 1981. Beginning of exocytosis captured by rapid-freezing of *Limulus* amebocytes. *J. Cell Biol.* **90:** 40–54.

Pittman, S., M. Geyp, M. Fraser, K. Ellem, A. Peaston, and C. Ireland. 1997. Multiple centrosomal microtubule organising centres and increased microtubule stability are early features of VP-16-induced apoptosis in CCRF-CEM cells. *Leuk. Res.* **21:** 491–499.

Pryzwansky, K. B., M. Schliwa, and K. R. Porter. 1983. Comparison of the three-dimensional organization of unextracted and Triton-extracted human neutrophilic polymorphonuclear leukocytes. *Eur. J. Cell Biol.* **30:** 112–125.

Shepro, D., F. A. Belamarich, and R. Branson. 1966. The fine structure of the thrombocyte in the dogfish (*Mustelus canis*) with special reference to microtubule orientation. *Anat. Rec.* **156:** 203–214.

Tahlin, F., and J. Levin. 1988. The fine structure of the amebocyte in the blood of *Limulus polyphemus.* II. The amebocyte cytoskeleton: a morphological analysis of native, activated, and endotoxin-stimulated amebocytes. *Biol. Bull.* **175:** 417–429.

Toh, Y., A. Mizutani, F. Tokunaga, T. Muta, and S. Iwanaga. 1991. Morphology of the granular hemocytes of the Japanese horseshoe crab *Tachypleus tridentatus* and immunocytochemical localization of clotting factors and antimicrobial substances. *Cell Tiss. Res.* **266:** 137–147.

Twersky, L. H., A. Bartley, N. Rayos, and W. D. Cohen. 1995. Immature erythroid cells with novel morphology and cytoskeletal structure in adult *Xenopus. Protoplasma* **185:** 37–49.

Volkov, Y., A. Long, and D. J. Kelleher. 1998. Inside the crawling T cell: leukocyte function-associated antigen-1 cross-linking is associated with microtubule-directed translocation of protein kinase C isoenzymes beta(I) and delta. *J. Immunol.* **161:** 6487–6495.

White, J. G., and C. C. Clawson. 1980. The surface-connected canalicular system of blood platelets—a fenestrated membrane system. *Am. J. Pathol.* **101:** 353–364.

Zigmond, S. H. 1978. Chemotaxis by polymorphonuclear leukocytes. *J. Cell Biol.* **77:** 269–287.